



An Immune-Related Prognostic Signature Predicts Overall Survival in Stomach Adenocarcinomas

Kangjie Zhou^{1,2†}, Nan Hu^{3†}, Yidong Hong^{3†}, Xueyu Wu³, Jingzhou Zhang³, Huan Lai³, Yang Zhang^{4*} and Fenglei Wu^{1,3*}

¹Department of Oncology, Lianyungang Clinical College of Nanjing Medical University/The First People's Hospital of Lianyungang, Lianyungang, China, ²Hospital of Xuzhou Medical University, The First People's Hospital of Lianyungang, Lianyungang, China, ³Department of Oncology, The Affiliated Lianyungang Hospital of Xuzhou Medical University/The First People's Hospital of Lianyungang, Lianyungang, China, ⁴Department of Obstetrics and Gynecology, The Affiliated Lianyungang Hospital of Xuzhou Medical University/The First People's Hospital of Lianyungang, Lianyungang, China

OPEN ACCESS

Edited by:

Chi-Chang Chang,
Chung Shan Medical University,
Taiwan

Reviewed by:

Fuyi Li,
The University of Melbourne, Australia
Yu-Hang Zhang,
Brigham and Women's Hospital,
United States

*Correspondence:

Yang Zhang
zhangyang19801027@njmu.edu.cn
Fenglei Wu
wufenglei1981@163.com

[†]These authors share first authorship

Specialty section:

This article was submitted to
Computational Genomics,
a section of the journal
Frontiers in Genetics

Received: 24 March 2022

Accepted: 18 April 2022

Published: 23 May 2022

Citation:

Zhou K, Hu N, Hong Y, Wu X, Zhang J,
Lai H, Zhang Y and Wu F (2022) An
Immune-Related Prognostic Signature
Predicts Overall Survival in
Stomach Adenocarcinomas.
Front. Genet. 13:903393.
doi: 10.3389/fgene.2022.903393

This study aimed to explore an immune response-related gene signature to predict the clinical prognosis and tumor immunity of stomach adenocarcinomas (STAD). Based on the expression and clinical data of STAD in the TCGA database, the immune cell infiltration status was evaluated using CIBERSORT and ESTIMATE methods. Samples were grouped into “hot” and “cold” tumors based on immune cell infiltration status and consensus clustering. The infiltration abundance of activated memory CD4 T cells and CD8 T cells had a significant effect on the overall survival of STAD patients. Among the three clusters, cluster 2 had a higher immune score and a significantly higher abundance of CD8 T cells and activated memory CD4 T cells were assigned as a hot tumor, while cluster 1 and 3 were assigned as a cold tumor. DEGs between hot and cold tumors were mainly enriched in immune-related biological processes and pathways. Total of 13 DEGs were related to the overall survival (OS). After the univariate and multivariable Cox regression analysis, three signature genes (PEG10, DKK1, and RGS1) was identified to establish a prognostic model. Patients with the high-risk score were associated with worse survival, and the risk score had an independent prognostic value. Based on TIMER online tool, the infiltration levels of six immune cell types showed significant differences among different copy number statuses of PEG10, DKK1, and RGS1. In this study, an immune-related prognostic model containing three genes was established to predict survival for STAD patients.

Keywords: Stomach adenocarcinomas, immune phenotype, immune infiltration, prognostic model, immunotherapy

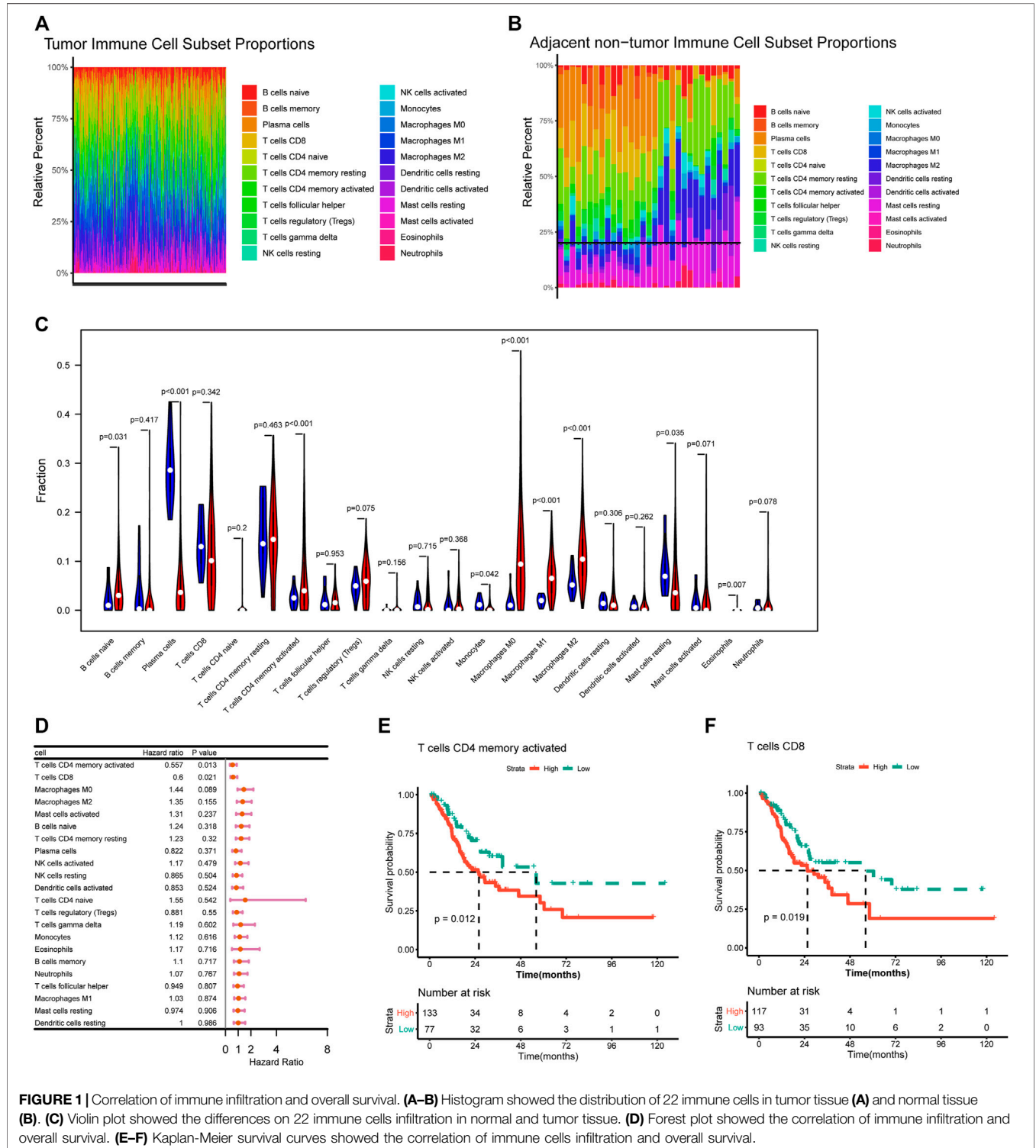
1 INTRODUCTION

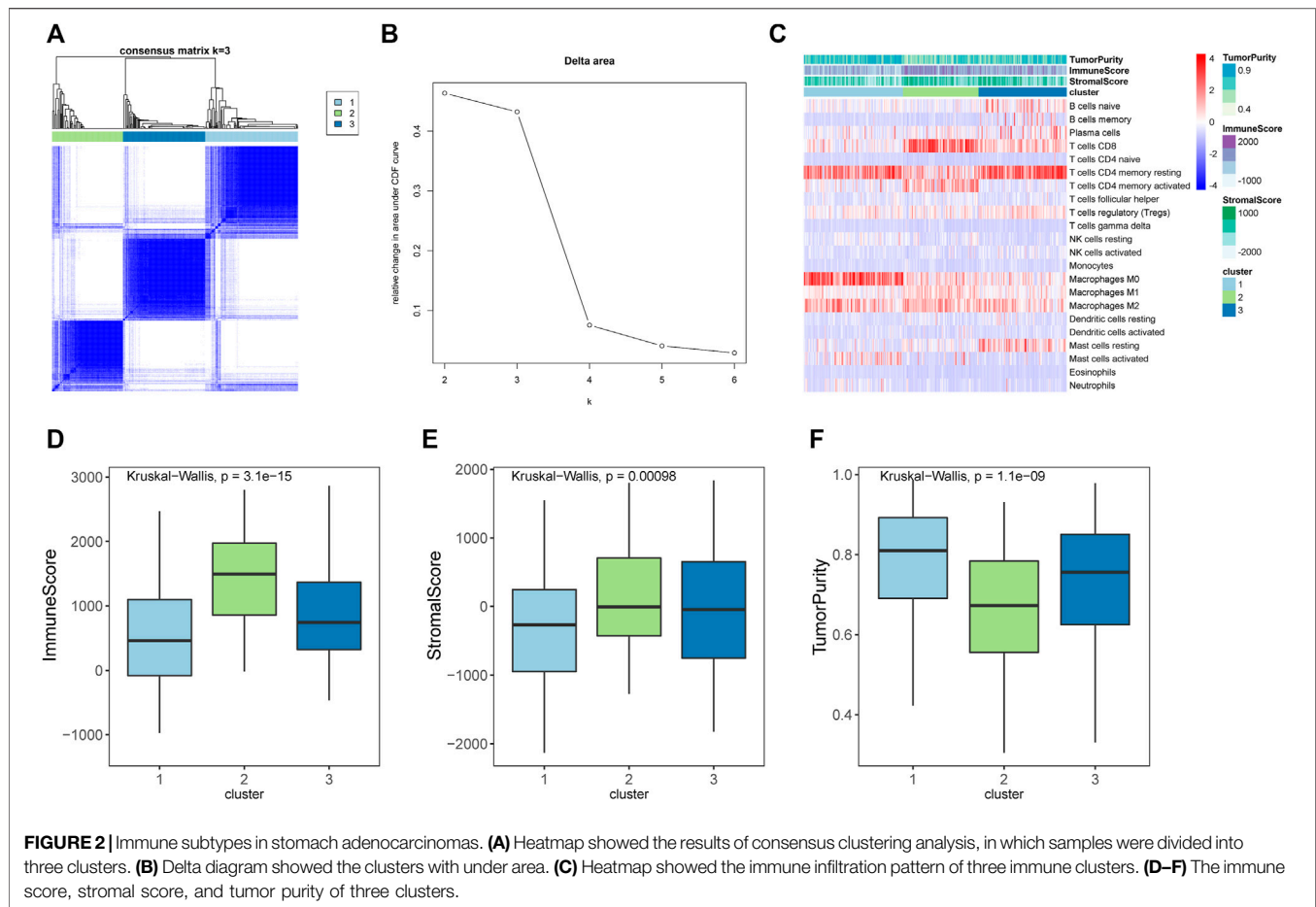
Stomach cancer is the fifth most common cancer worldwide and the third leading cause of cancer death (Bray et al., 2018). The new cases of gastric cancer in China account for 47% of the total number of gastric cancer in the world every year, and more than 60% of the patients are locally advanced or advanced at the time of treatment, and the 5-year survival rate is less than 30% (Chen et al., 2016; Feng et al., 2019). The annual death rate of gastric cancer in China has dropped from 3.8% to 2.3% over the past decade due to advances in diagnosis and treatment technology (Gao and Wu, 2019). Stomach adenocarcinomas (STAD) are the most common type of stomach carcinomas

(Rima et al., 2020). Conventional treatments such as surgery, chemotherapy, and radiotherapy have limited efficacy for stomach cancer. Although molecularly targeted drugs such as Trastuzumab, Apatinib, and ramucirumab have been approved for stomach cancer successively, the targeted therapy of stomach cancer is still far behind lung cancer, breast cancer, colon cancer,

and other common tumors (de Haas et al., 2014; Taberero et al., 2018).

Tumor cells can escape the surveillance of immune response through various mechanisms, one of the most important mechanisms is immune checkpoint mediated co-inhibitory signaling pathway (Waldman et al., 2020). The high





expression of various checkpoint proteins on T cells in stomach cancer tissues, including CTLA-4, IDO, LAG3, and PD-1, suggests that they have the phenotype of T cell immune exhaustion and the tumor microenvironment is in an immunosuppressive state (Taieb et al., 2018; Vrána et al., 2018; Li K. et al., 2021). Some stomach cancer tumor cells also have a high mutation load, especially those with high microsatellite instability, which can express abundant tumor antigens and thus initiate a stronger immune response (van Velzen et al., 2020). Moreover, checkpoint proteins PD-1 and PD-L1 were up-regulated in tumors with high microsatellite instability (Llosa et al., 2015), which showed well response to PD-1 inhibitors (Le et al., 2015). But not all stomach cancer patients benefit from immunotherapy alone. Therefore, it is necessary to explore the immunophenotypic classification of stomach cancer to screen the dominant population that may benefit from immunotherapy and to identify suitable biomarkers for monitoring treatment efficacy.

It has been demonstrated that the “hot” tumor phenotype has high response rates to immune checkpoint inhibitors, in which the immune cell infiltration in the tumor microenvironment are mainly characterized, while tumor with low immune infiltrations is regarded as “cold” tumor (Maleki Vareki, 2018). Such tumor classification can partly explain the response to immune

checkpoint inhibitors treatment. Current bioinformatics technology enabled us to characterize the immune infiltration pattern and the immune score of tumors. Therefore, we intended to divide STAD samples into hot and cold tumors based on the data in TCGA and to identify signature genes that are associated with the hot and cold tumors for prognostic model establishment.

2 MATERIALS AND METHODS

2.1 Data Acquisition

The FPKM RNA-sequencing data and clinical phenotype data of STAD were downloaded from The Cancer Genome Atlas (TCGA) database, including 350 tumor samples and 31 adjacent normal samples. Somatic mutation data of STAD was also acquired from the TCGA database. The preprocessed series matrix of GSE19188 was downloaded from Gene Expression Omnibus (GEO) database, which involves 300 STAD samples and 100 normal samples. Data were annotated based on the annotation files (hg38, V22) provided in the Gencode database, with Ensembl-ID converting to gene symbol. The mean value was considered as the final expression value when multiple Ensembl-ID matched to one gene symbol.

2.2 Characterization of Immune Infiltration

The infiltration abundance of 22 immune cells of STAD was estimated by using the CIBERSORT algorithm based on the LM22 gene expression characteristic provided on the CIBERSORT website with parameters set as perm = 100 and QN = F. Samples with $p < 0.05$ were screened for estimating the infiltration landscape of STAD and normal samples. The stromal score, immune score, and tumor purity of STAD samples were calculated by using the ESTIMATE package in R. In addition, the infiltration abundance of six immune cell types was estimated by using the TIMER online tool (<https://cistrome.shinyapps.io/timer/>).

2.3 Consensus Clustering Analysis

Based on the infiltration abundance of 22 immune cells, STAD samples were grouped into different clusters by using the consensuscluster Plust algorithm (version 1.50.0) with parameters set as maxK = 6, pItem = 0.8, clusterAlg = "hc" and distance = "pearson". The cumulative distribution function (CDF) was used to identify the most reasonable number of clusters.

2.4 Hot and Cold Tumors

Based on immune infiltration, immune score, and consensus clustering subtypes, STAD samples were categorized into hot tumors and cold tumors. Kaplan-Meier (KM) survival analysis with log-rank test was performed using the survival package (version 3.2-7). Tumor mutation burden (TMB) of hot and cold tumors was analyzed using the Maftools package (version 2.0.16) based on the somatic mutation data.

2.5 Differential Expression Analysis and Function Enrichment

The differentially expressed genes (DEGs) between hot tumor and cold tumor were screened based on the t -test provided in the Limma package (version 3.10.3) with cut-off values of Benjamini-Hochberg (BH) multiple tests adjusted $p < 0.05$ and $|\log_2FC| > 0.585$. Gene ontology annotation terms and KEGG pathways were enriched for DEGs using the over-representation analysis (ORA) method provided by the gprofiler online tool (<https://biit.cs.ut.ee/gprofiler/convert>) with a cut-off value of BH adjusted $p < 0.05$.

TABLE 1 | The differences on clinical phenotype between hot and cold tumors.

	Cool tumor (N = 249)	Hot tumor (N = 101)	<i>p</i> -value
Gender			
Female	78 (31.3%)	41 (40.6%)	0.116
Male	162 (65.1%)	56 (55.4%)	
Missing	9 (3.6%)	4 (4.0%)	
Age (years)			
<60	73 (29.3%)	32 (31.7%)	0.731
≥60	165 (66.3%)	64 (63.4%)	
Missing	11 (4.4%)	5 (5.0%)	
Stage			
Stage I	34 (13.7%)	11 (10.9%)	0.285
Stage II	69 (27.7%)	38 (37.6%)	
Stage III	98 (39.4%)	39 (38.6%)	
Stage IV	27 (10.8%)	7 (6.9%)	
Missing	21 (8.4%)	6 (5.9%)	
T			
T1	13 (5.2%)	2 (2.0%)	0.349
T2	56 (22.5%)	18 (17.8%)	
T3	106 (42.6%)	50 (49.5%)	
T4	63 (25.3%)	25 (24.8%)	
Missing	11 (4.4%)	6 (5.9%)	
N			
N0	68 (27.3%)	31 (30.7%)	0.24
N1	62 (24.9%)	29 (28.7%)	
N2	55 (22.1%)	13 (12.9%)	
N3	46 (18.5%)	22 (21.8%)	
Missing	18 (7.2%)	6 (5.9%)	
M			
M0	215 (86.3%)	88 (87.1%)	0.397
M1	18 (7.2%)	4 (4.0%)	
Missing	16 (6.4%)	9 (8.9%)	
G			
G1	9 (3.6%)	0 (0%)	<0.001
G2	97 (39.0%)	23 (22.8%)	
G3	126 (50.6%)	73 (72.3%)	
Missing	17 (6.8%)	5 (5.0%)	

2.6 Co-expression of DEGs With N6-Methyladenosine (m6A) Regulator Genes

Expression of m6A regulator genes (writers: METTL3, METTL14, METTL15, WTAP, VIRMA, RBM15, RBM15B, KIAA1429, ZC3H13; erasers: FTO, ALKBH5; readers: RBMX, YTHDC1, YTHDC2, IGF2BP1, IGF2BP2, IGF2BP3, YTHDF1, YTHDF2, YTHDF3, HNRNPA2B1, HNRNPC) were extracted from TCGA dataset. Then, the Pearson correlation coefficient (PCC) of the expression level of m6A regulator genes and DEGs was calculated based on the cor test in R 3.6.1 (<http://77.66.12.57/R-help/cor.test.html>) with a cut-off value of the absolute value of correlation coefficient > 0.15 and $p < 0.05$.

2.7 Construction of Prognostic Risk Model

KM survival analysis was performed for all DEGs with samples dividing into high-expression and low-expression by median value, and genes with log-rank $p < 0.05$ were regarded as prognostic genes. All the STAD samples were randomly divided into the training-set and validation-set with a ratio of 5:5. In training-set, the univariate Cox regression analysis in the survival package was performed for KM prognostic genes and genes with $p < 0.05$ were considered signature genes for model construction. Multivariable Cox regression analysis was used to calculate the prognostic coefficient for signature genes. Then, the prognostic risk model was established according to the formula: Risk score = \sum Coef gene \times Exp gene, of which Coef and Exp refer to the prognostic coefficient and expression value of each signature gene, respectively.

After calculating the risk score, samples were assigned into high- and low-risk groups based on the median risk score. KM survival analysis was performed to detect the survival differences between the two risk groups. GSE19188 was used as an external dataset to validate the prognostic model.

2.8 Protein Expression of Signature Genes

In order to investigate the protein expression of signature genes in STAD, the immunohistochemistry images of STAD

were acquired from The Human Protein Atlas (<http://www.proteinatlas.org>) database.

2.9 Statistical Analysis

The correlations of immune cells infiltration abundance with overall survival (OS) were analyzed based on univariate Cox regression analysis in the survival package (version3.2-7). The differences in infiltration abundance of each immune cell type between STAD and normal samples were compared using WilcoxTest. The differences in stromal score, immune

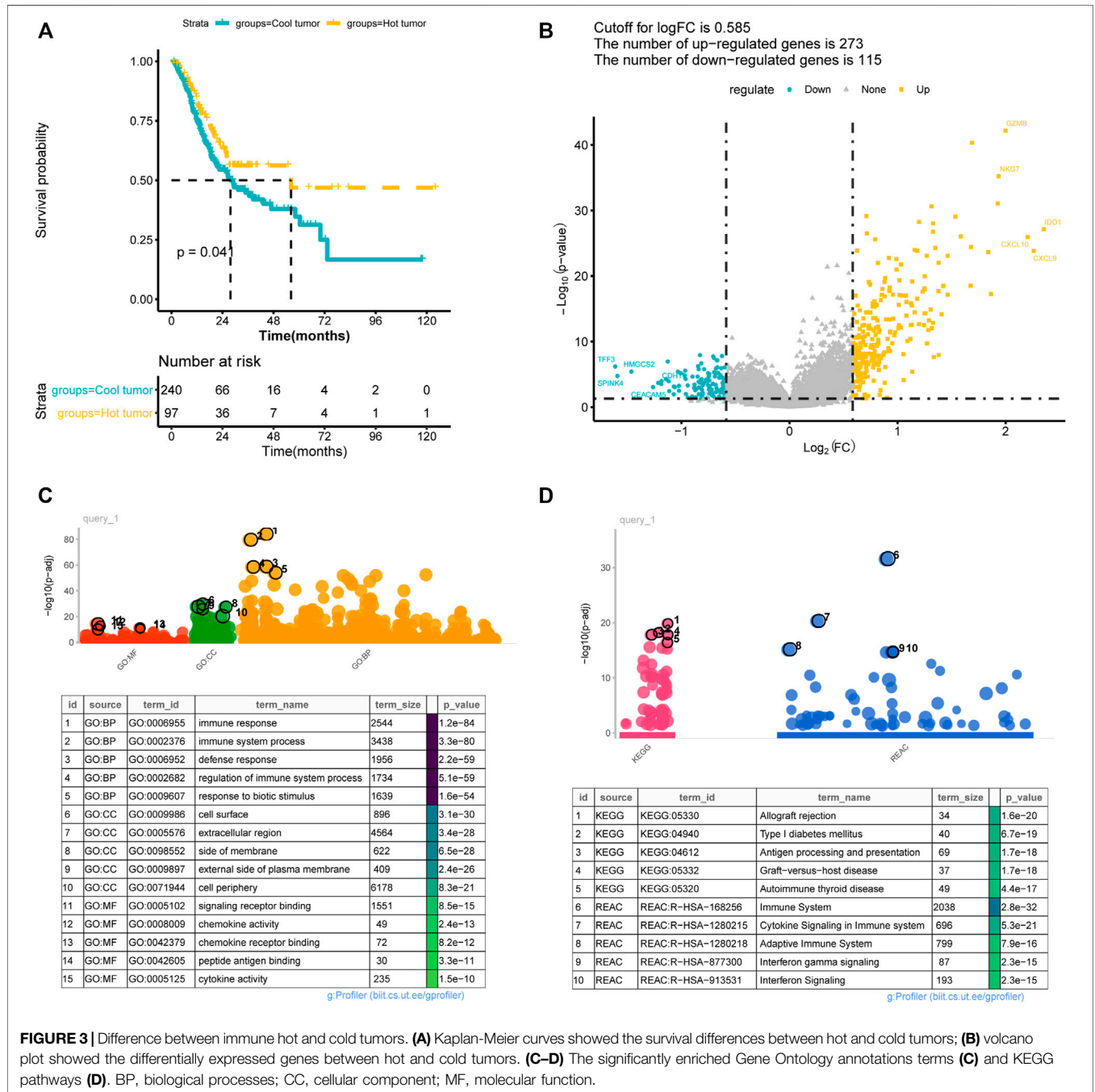


FIGURE 3 | Difference between immune hot and cold tumors. **(A)** Kaplan-Meier curves showed the survival differences between hot and cold tumors; **(B)** volcano plot showed the differentially expressed genes between hot and cold tumors. **(C-D)** The significantly enriched Gene Ontology annotations terms **(C)** and KEGG pathways **(D)**. BP, biological processes; CC, cellular component; MF, molecular function.

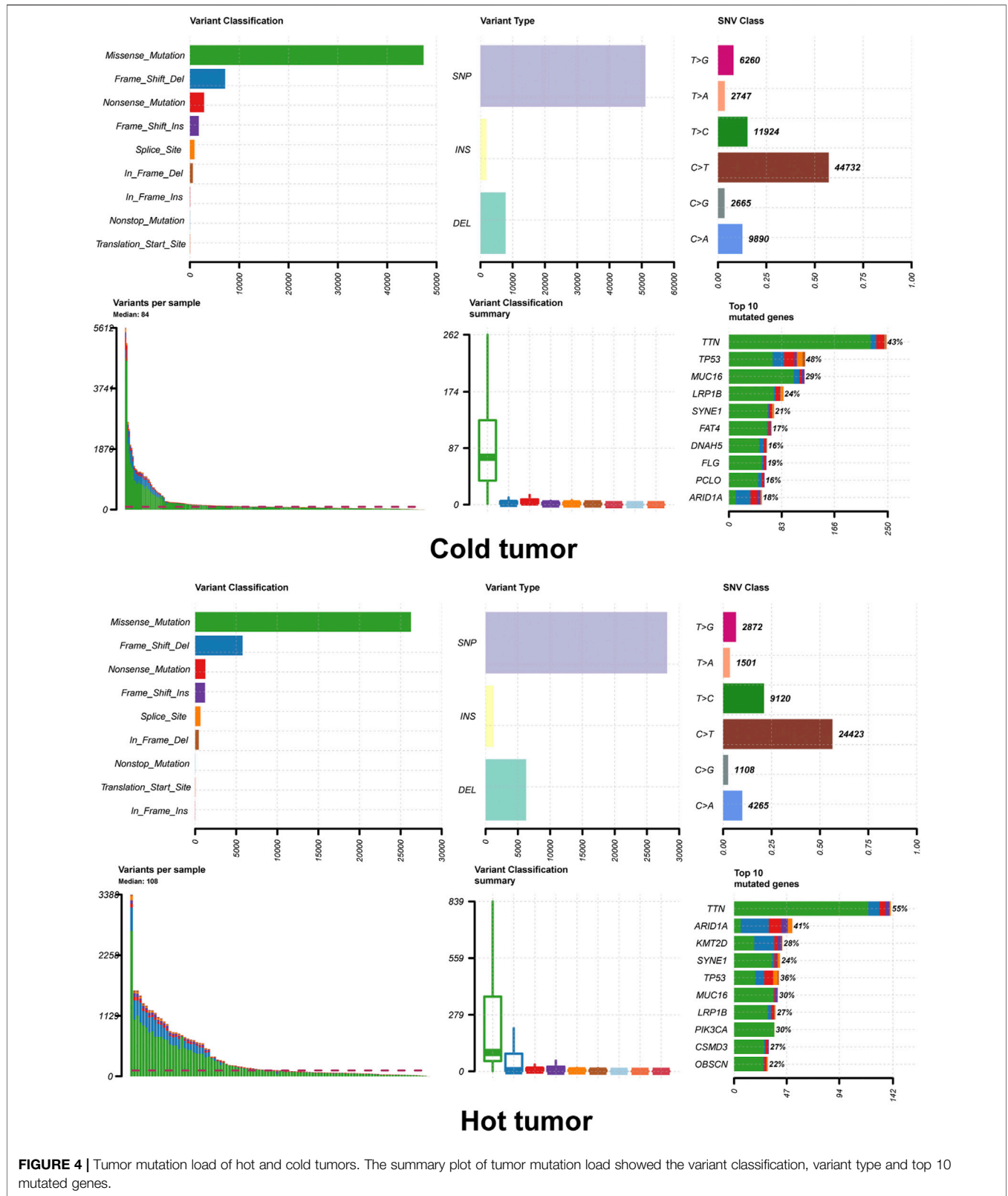


FIGURE 4 | Tumor mutation load of hot and cold tumors. The summary plot of tumor mutation load showed the variant classification, variant type and top 10 mutated genes.

TABLE 2 | Results of univariate Cox regression analysis.

Symbol	Hazard ratio	p value
PEG10	1.224(1.091–1.372)	0.001
DKK1	1.161(1.039–1.297)	0.009
RGS1	1.240(1.033–1.488)	0.021
COL10A1	1.124 (0.988–1.278)	0.075
ENTPD8	0.837 (0.688–1.019)	0.076
FUT6	0.873 (0.735–1.039)	0.126
PYCARD	0.812 (0.612–1.079)	0.151
PTPRN2	0.890 (0.749–1.056)	0.182
MICB	0.848 (0.643–1.119)	0.244
BATF2	0.897 (0.745–1.079)	0.248
TK1	0.856 (0.652–1.125)	0.265
MMP12	0.972 (0.871–1.085)	0.617
PSMB10	0.960 (0.746–1.235)	0.75

score, and tumor purity among different immune subtypes were compared by using a *t*-test. The differences in clinical phenotype (including age, gender, TNM stage, pathologic-stage, and tumor grades) between hot and cold tumors were compared using the chi-square test. Univariate and multivariable Cox regression analyses were performed to evaluate the independent predictive value of the prognostic model. Statistical difference was presented with *p* < 0.05.

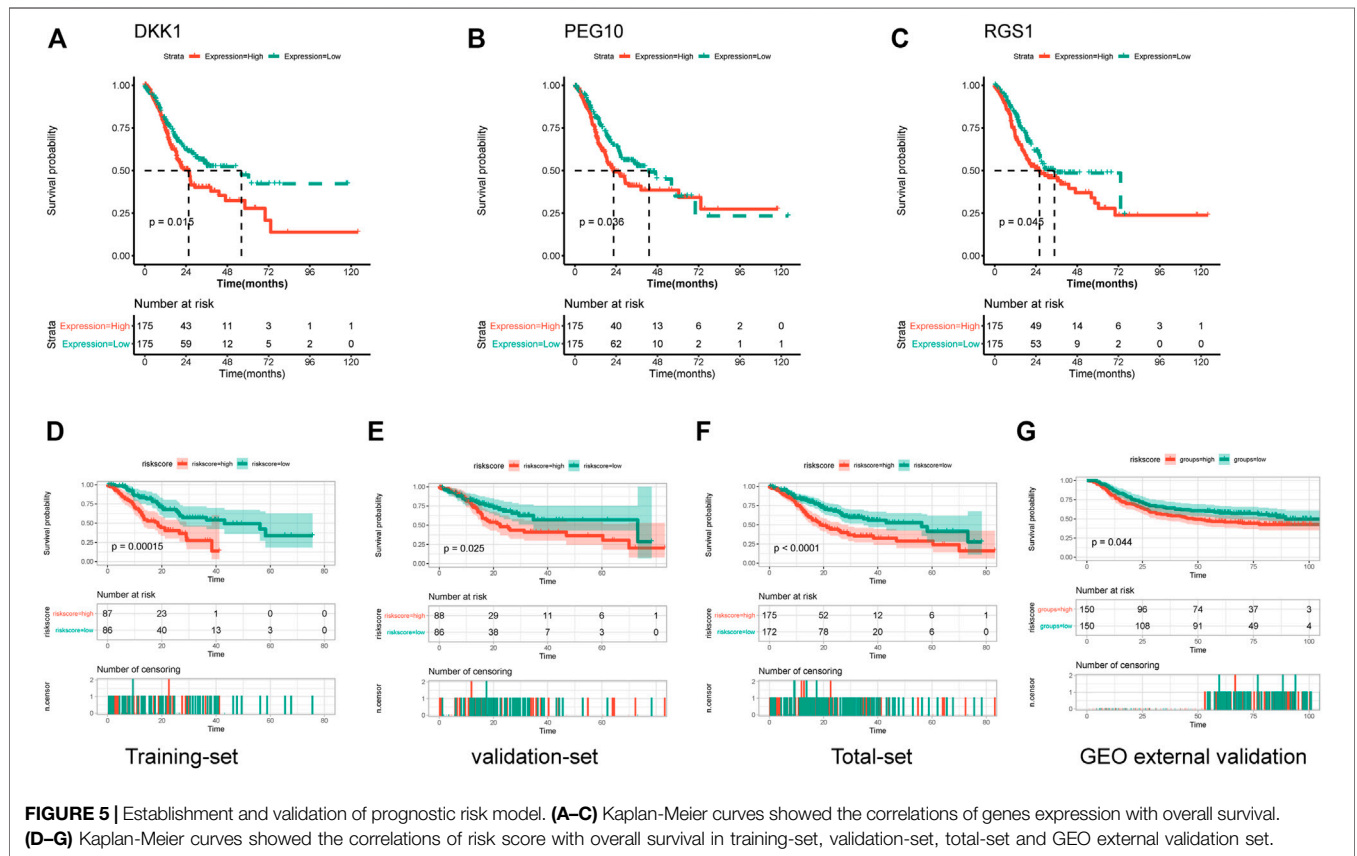
3 RESULTS

3.1 Immune Infiltration Landscape in Tumor and Normal Samples

The proportion of 22 immune infiltration cells in the tumor and normal samples was evaluated. As shown in **Figures 1A,B**, the infiltration proportion varied among different cell types, and there were also differences in infiltration proportion for the same cell type among samples. The infiltration abundance between tumor and normal samples was also compared. It could be seen that tumor samples showed a significantly higher infiltration abundance of activated memory CD4 T cells, naive B cells, macrophages M0/M1/M2, and eosinophils, while normal samples showed a significantly higher infiltration abundance of plasma cells and resting mast cells (**Figure 1C**).

3.2 Correlations of Immune Infiltration With Overall Survival

The correlations of immune cells infiltration abundance with OS were analyzed based on univariate Cox regression analysis in the survival package, and the results showed that activated memory CD4 T cells (HR = 0.557, *p* = 0.013) and CD8 T cells (HR = 0.6, *p* = 0.021) had significant effect to OS of STAD patients (**Figure 1D**). Further survival analysis indicated that higher



infiltration abundance of activated memory CD4 T cells and CD8 T cells were associated with shorter survival time (Figures 1E,F).

3.3 Immune Subtypes of Stomach Adenocarcinomas

To explore whether the STAD samples could be grouped into different clusters based on the immune infiltration pattern, a consensus clustering analysis was performed. Results indicated that STAD samples could be grouped into three clusters (Figures 2A,B). The distribution of immune cells in different clusters were shown in Figure 2C, cluster 2 had significantly higher abundance of CD8 T cells and activated memory CD4 T cells. Cluster 1 had significantly higher abundance of resting memory CD4 T cells and macrophages M0, and cluster 3 had a significantly higher abundance of resting memory CD4 T cells. Further ESTIMATE analysis suggested that cluster 2 had higher immune-score and stromal-score, while showed lower tumor-purity than other clusters (Figures 2D-F). Considering that cluster 2 had higher immune-score and a significantly higher abundance of CD8 T cells and activated memory CD4 T cells, which were important immune cells for targeting cancer in immunotherapy, we assigned cluster 2 as hot tumors. While cluster 1 and 3 had a significantly higher abundance of resting memory CD4 T cells and decreased abundance of CD8 T cells, therefore we assigned cluster 1 and 3 as cold tumors.

3.4 Clinical Correlations of Hot and Cold Tumors

The differences in clinical phenotype (including age, gender, TNM stage, pathologic-stage, and tumor grades) between hot and cold tumors were compared using the chi-square test. As shown in Table 1, there were no differences on age, gender, TNM stage, or pathologic-stage between hot and cold tumors, while there had significant differences in tumor grades. The cold tumor contained more proportion of lower grade tumors (grade 1–2, 42.6% vs 22.8%) than the hot tumor, while the hot tumor contained more proportion of higher-grade tumors

(grade 3, 72.3% vs 50.6%) than the cold tumor. Survival analysis showed that hot tumors were associated with longer survival (Figure 3A).

3.5 Differential Expression Between Hot and Cold Tumors

A total of 388 DEGs were screened between hot and cold tumors, of which 273 genes were up-regulated and 115 genes were down-regulated (Figure 3B). Further functional enrichment indicated that these DEGs were significantly involved in immune-related biological processes, such as immune response, immune system process, and regulation of immune system process (Figure 3C). DEGs were also significantly enriched in immune-related pathways, such as antigen processing and presentation; immune system, cytokine signaling in the immune system, adaptive immune system, and interferon signaling (Figure 3D). TMB has been regarded as a prognostic and predictive biomarker for immune checkpoint inhibitors therapy (McNamara et al., 2020). Therefore, we analyzed the TMB patterns, and similar TMB patterns were found between hot and cold tumors (Figure 4). Missense mutation was the most frequent variant classification, single nucleotide polymorphism (SNP) accounted for the most frequent variant types. However, there were significant differences in the top 10 mutated genes and their mutation frequency between hot and cold tumors. The hot tumor had a higher mutation frequency of OBSCN, CSMD3, PIK3CA, and KMT2D, which were not found in the top 10 mutated genes in the cold tumor. The cold tumor had a higher mutation frequency of PCLO, FLG, DNAH5, and FAT4, which were not found in the top 10 mutated genes in the hot tumor. In addition, the mutation frequency for commonly mutated genes showed differences, for example, ARID1A (41% vs 18% in hot and cold tumors).

3.6 Identification of Signature Genes for Prognostic Model Establishment

In order to investigate the prognostic value of these DEGs, KM survival analysis was performed, and 13 genes were found to be associated with the overall survival of patients (Supplementary

TABLE 3 | Univariate and multivariables Cox regression analysis for clinical factors.

Clinical characteristics	Univariables cox		Multivariables cox	
	Hazard ratio	p Value	Hazard ratio	p Value
pathologic_N	1.328(1.145–1.540)	0	0.107	1.208 (0.960–1.520)
Stage	1.494(1.219–1.830)	0	0.696	1.085 (0.722–1.631)
RiskScore	1.969(1.410–2.751)	0	0.001	1.906(1.310–2.775)
pathologic_T	1.291(1.051–1.586)	0.015	0.381	1.138 (0.852–1.520)
pathologic_M	1.959(1.103–3.481)	0.022	0.523	1.294 (0.586–2.856)
Grade	1.383(1.005–1.904)	0.047	0.394	1.174 (0.812–1.699)
Age	1.446 (0.995–2.102)	0.053		
Groups	0.694 (0.475–1.013)	0.058		
Gender	1.325 (0.930–1.887)	0.119		

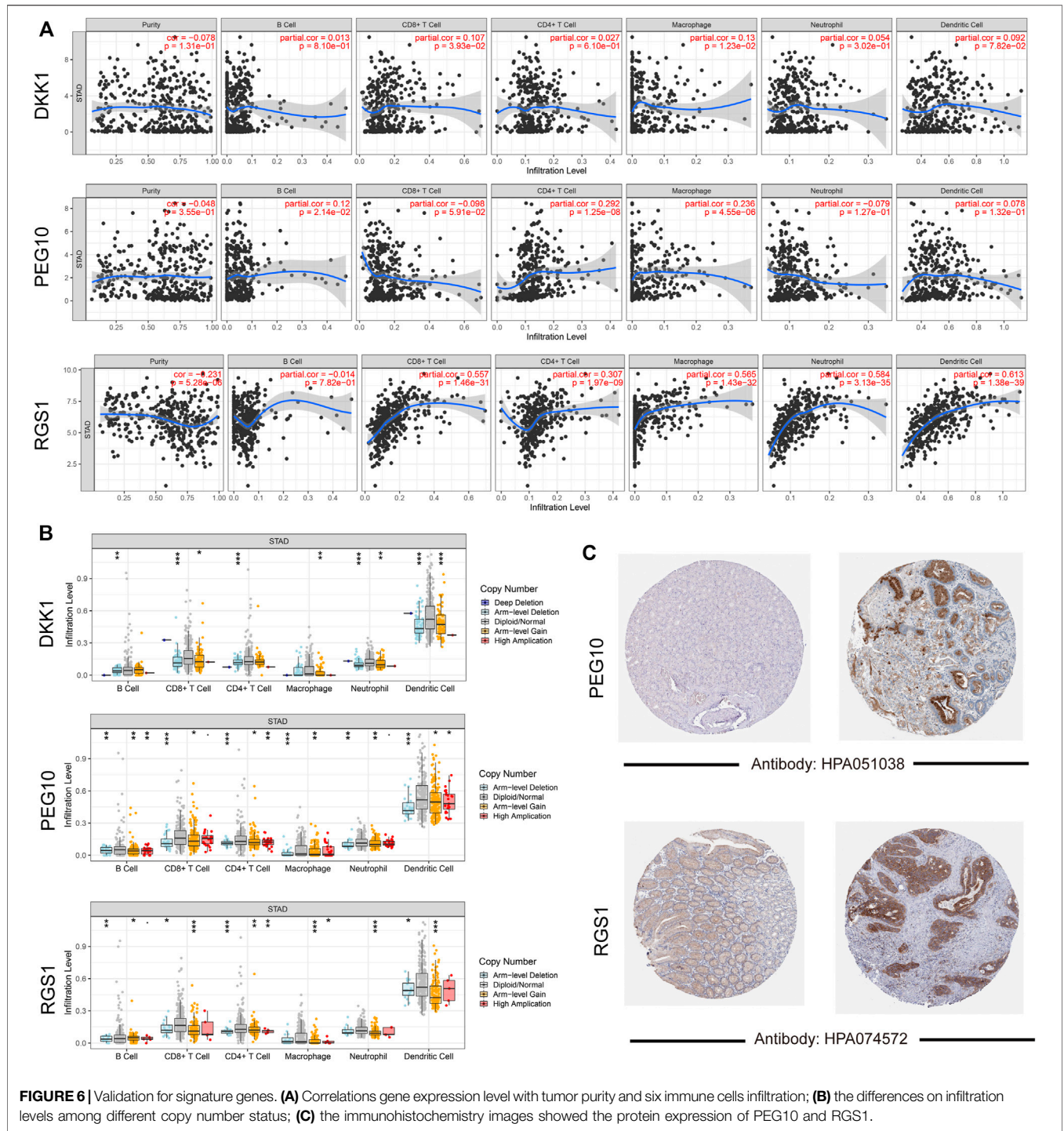


FIGURE 6 | Validation for signature genes. **(A)** Correlations gene expression level with tumor purity and six immune cells infiltration; **(B)** the differences on infiltration levels among different copy number status; **(C)** the immunohistochemistry images showed the protein expression of PEG10 and RGS1.

Table S1). The associations of these prognostic genes with M6A regulator genes were investigated, and all 13 prognostic genes showed co-expression with m6A regulator genes (**Supplementary Figure S1**), indicating that these genes might be regulated by m6A methylated modification. Univariate Cox regression analysis was performed for these 13 prognostic genes, and three signature genes (PEG10, DKK1, and RGS1) were identified to have a significant effect on the overall survival of

patients (**Table 2**). These three genes were identified as risk factors for survival with a hazard ratio >1. Consistently, KM survival analysis indicated that high expression of PEG10, DKK1, and RGS1 were associated with poor survival (**Figures 5A–C**). After calculating the prognostic coefficient for signature genes using multivariable Cox regression analysis, the prognostic model was established with the formula of Risk score = PEG10*0.002 + RGS1*0.018 + DKK1* 0.074. Survival analysis indicated that the

risk score could stratify STAD patients, of which patients in the high-risk group were found to have a shorter survival time than that of the low-risk group in both training-set, validation-set, total-set, and GEO external validation dataset (Figures 5D–G). Additionally, the risk score was identified as a prognostic factor independent from other clinical phenotype factors in STAD (Table 3).

3.7 Association of Signature Genes Expression With Immune Infiltration Levels

The associations of signature gene expression with immune infiltration levels in STAD were analyzed using the TIMER online tool. As shown in Figure 6A, expression of RGS1 showed strong positive correlations with the infiltration levels of CD8⁺ T cells, CD4⁺ T cells, macrophage, neutrophil, and dendritic cells ($r > 0.3$ and $p < 0.05$). PEG10 expression showed weak positive correlations with the infiltration levels of CD4⁺ T cells and macrophages ($p < 0.05$). The infiltration levels of all these six immune cell types showed significant differences among different copy number statuses of three signature genes (Figure 6B). Additionally, to detect the protein expression of signature genes in STAD, the immunohistochemistry images of STAD were acquired from the HPA database. Consistently, protein expression of PEG10 and RGS1 showed significantly high expression in tumor tissue than in the normal tissue (Figure 6C). No immunohistochemistry images for DKK1 were found.

4 DISCUSSION

In recent years, the attention to tumor immunotherapy is rapidly increasing, and the theory and practice of immunotherapy for stomach cancer have also achieved good results, bringing hope to patients with advanced cancer, but there are still many obstacles to overcome. For example, some patients showed continued response after a short period of ipilimumab treatment. However, some patients respond well to initial immunotherapy but relapse after a period of time (Bang et al., 2017; Janjigian et al., 2018). Therefore, it is necessary to explore the immune phenotype classification of stomach cancer and screen the dominant population that may benefit from immunotherapy.

In the current study, the immune infiltration landscape of STAD was investigated. Various immune cell types showed significant differences in infiltrating abundance between tumor and normal samples. Tumor samples showed significantly higher infiltration abundance of activated memory CD4 T cells, naive B cells, macrophages, and eosinophils, while normal samples showed significantly higher infiltration abundance of plasma cells and resting mast cells. In addition, activated memory CD4 T cells and CD8 T cells were found to have a significant effect on the OS of STAD patients. This emphasized that the immune infiltrating status had the ability to reflect the prognosis of patients. The purpose of tumor immunotherapy is to promote the activity of cytotoxic T lymphocytes (CTLs) within the tumor and to

establish durable and efficient anti-tumor immunity (Maher and Davies, 2004). CD4⁺ T cells can not only kill tumor cells directly in an IFN- γ -dependent manner but also maintain and promote the survival of CD8⁺ T cells through activation of CD8⁺ T cells, generation of memory CTLs response, and so on (Borst et al., 2018). Tumor-infiltrating lymphocytes (TIL) is a heterogeneous lymphocyte group that has an anti-tumor effect on the tumor, and CD8⁺ T cells are the main effector cells (Farhood et al., 2019; Raskov et al., 2021). The loss of TILs function in the tumor microenvironment is the main factor leading to tumor progression and failure of cellular immunotherapy (Zhang et al., 2019; Lin et al., 2020). Therefore, simultaneously activating CD4⁺ T cells and CD8⁺ T cells is an ideal strategy for immunotherapy.

Based on the immune infiltration pattern, the STAD samples were grouped into three clusters in consensus clustering analysis, of which Cluster two was mainly enriched by a higher abundance of CD8 T cells and activated memory CD4 T cells, and had high immune-score calculated by ESTIMATE algorithm. Therefore Cluster 2 was defined as a hot tumor. While cluster 1 and 3 had a significantly higher abundance of resting memory CD4 T cells and decreased abundance of CD8 T cells as well as a lower immune score, therefore we assigned cluster 1 and 3 as a cold tumor. The differences at the transcriptional level between hot and cold tumors were further investigated. Consistently, genes that were differentially expressed between hot and cold tumors were mainly enriched in immune-related biological processes and pathways, such as antigen processing and presentation; immune system, cytokine signaling in the immune system, adaptive immune system, and interferon signaling.

From these DEGs, three signature genes associated with overall survival were identified, including PEG10, DKK1, and RGS1. PEG10 encodes paternally expressed gene 10, and has been demonstrated to be highly expressed in various tumors, functioning as an oncogene involved in apoptosis, proliferation, and metastasis of tumors (Xie et al., 2018). PEG10 expression has been linked to worse prognosis and tumor progression or recurrence in endometrial cancer (Zhang et al., 2021), hepatocellular carcinoma (Bang et al., 2015), oral squamous cell carcinoma (Sharan Singh et al., 2017), showing potential predictive and prognostic ability as a biomarker (Ge et al., 2018). PEG10 knockdown showed an anti-tumor effect in stomach cancer by inhibiting proliferation, migration, and invasion (Wang et al., 2018). DDK1 is a dickkopf-related protein, also known as an inhibitor one of beta-catenin-dependent Wnt signaling. Elevated expression of DKK1 has been reported in different tumors (Betella et al., 2020). Expression of DKK1 in both serum and tissue levels has been reported to be a biomarker in diagnosis and predicting survival and tumor recurrence in stomach cancer (Lee et al., 2012; Liu et al., 2016; Hong et al., 2018). In addition, DDK1 has been linked to T-DM1 resistance in STAD (Li et al., 2018). Moreover, DKN-01, an IgG4 monoclonal antibody targeting DKK1 has been demonstrated to have therapeutic benefits in gastroesophageal malignancies (Wall et al., 2020), indicating the potential of DKK1 in cancer therapy. RGS1, a regulator of G protein signaling 1, expression has been reported to have a significant effect on the

survival of stomach cancer, and is associated with the differentiation degree of tumor (Li S. et al., 2021). RGS is linked to various immune-mediated diseases. RGS1 is highly expressed in certain B cells, and deeply affects the directed migration of lymphoid cells (Moratz et al., 2000). Dendritic cells transfected with RGS1 can generate RGS1-specific cytotoxic T cells (Grünebach et al., 2008). Also, RGS1 has been reported to affect the frequency of follicular helper T cells (Caballero-Franco and Kissler, 2016). This was consistent with our findings that expression of RGS1 showed strong positive correlations with the infiltration levels of CD8⁺ T cells, CD4⁺ T cells, macrophage, neutrophil, and dendritic cells. Limitations of our study are as follows: first, our prediction model was constructed and validated with data from the TCGA database and GEO based on the “cold” and “hot” tumors. The use of this model in a real clinical setting remains controversial. More studies are still required to confirm our observation. Besides, the testing result of mRNA expression level is not stable. In the future, we will further verify this prediction model at the protein expression level.

5 CONCLUSION

A three-gene-based immune-related prognostic model was established, which could stratify STAD patients well. Patients with the high-risk score were associated with worse survival, and the risk score had an independent prognostic value. Our model contributed to exploring the immune phenotype classification of STAD and screening the dominant population that may benefit from immunotherapy.

DATA AVAILABILITY STATEMENT

The original contributions presented in the study are included in the article/**Supplementary Material**, further inquiries can be directed to the corresponding authors.

REFERENCES

- Bang, H., Ha, S. Y., Hwang, S. H., and Park, C.-K. (2015). Expression of PEG10 Is Associated with Poor Survival and Tumor Recurrence in Hepatocellular Carcinoma. *Cancer Res. Treat.* 47, 844–852. doi:10.4143/crt.2014.124
- Bang, Y.-J., Cho, J. Y., Kim, Y. H., Kim, J. W., Di Bartolomeo, M., Ajani, J. A., et al. (2017). Efficacy of Sequential Ipilimumab Monotherapy Versus Best Supportive Care for Unresectable Locally Advanced/Metastatic Gastric or Gastroesophageal Junction Cancer. *Clin. Cancer Res.* 23, 5671–5678. doi:10.1158/1078-0432.ccr-17-0025
- Betella, I., Turbitt, W. J., Szul, T., Wu, B., Martinez, A., Katre, A., et al. (2020). Wnt Signaling Modulator DKK1 as an Immunotherapeutic Target in Ovarian Cancer. *Gynecol. Oncol.* 157, 765–774. doi:10.1016/j.ygyno.2020.03.010
- Borst, J., Ahrends, T., Bąbala, N., Melief, C. J. M., and Kastanmüller, W. (2018). CD4(+) T Cell Help in Cancer Immunology and Immunotherapy. *Nat. Rev. Immunol.* 18, 635–647. doi:10.1038/s41577-018-0044-0
- Bray, F., Ferlay, J., Soerjomataram, I., Siegel, R. L., Torre, L. A., and Jemal, A. (2018). Global Cancer Statistics 2018: GLOBOCAN Estimates of Incidence and Mortality

ETHICS STATEMENT

Ethical review and approval was not required for the study on human participants in accordance with the local legislation and institutional requirements. Written informed consent from the patients/participants or patients/participants' legal guardian/next of kin was not required to participate in this study in accordance with the national legislation and the institutional requirements.

AUTHOR CONTRIBUTIONS

Conception and design of the research: FW and YZ; draft the manuscript: KZ and NH; Acquisition of data: XW and HL; Analysis and interpretation of data: YH and JZ; Obtaining funding: FW and NH; All authors read and approved the final manuscript.

FUNDING

This work was supported by the National Natural Science Foundation of China (Grant No. 81802347), Jiangsu Provincial Social Development Project (Grant No. BE2019693), the Clinical research project of Wu Jieping Foundation (Grant No. 320.6750.19058), and the foundation of Lianyungang City 521 (Grant No. LYG06521202124).

SUPPLEMENTARY MATERIAL

The Supplementary Material for this article can be found online at: <https://www.frontiersin.org/articles/10.3389/fgene.2022.903393/full#supplementary-material>

Supplementary Figure S1 | Expression correlations of prognostic genes and m6A regulator genes. **p<0.01

Supplementary Table S1 | The 13 prognostic related genes identified by Kaplan-Meier survival analysis.

Worldwide for 36 Cancers in 185 Countries. *CA Cancer J. Clin.* 68, 394–424. doi:10.3322/caac.21492

Caballero-Franco, C., and Kissler, S. (2016). The Autoimmunity-Associated Gene RGS1 Affects the Frequency of T Follicular Helper Cells. *Genes Immun.* 17, 228–238. doi:10.1038/gene.2016.16

Chen, W., Zheng, R., Baade, P. D., Zhang, S., Zeng, H., Bray, F., et al. (2016). Cancer Statistics in China, 2015. *CA Cancer J. Clin.* 66, 115–132. doi:10.3322/caac.21338

de Haas, S., Delmar, P., Bansal, A. T., Moisse, M., Miles, D. W., Leigh, N., et al. (2014). Genetic Variability of VEGF Pathway Genes in Six Randomized Phase III Trials Assessing the Addition of Bevacizumab to Standard Therapy. *Angiogenesis* 17, 909–920. doi:10.1007/s10456-014-9438-1

Farhood, B., Najafi, M., and Mortezaee, K. (2019). CD8(+) Cytotoxic T Lymphocytes in Cancer Immunotherapy: A Review. *J. Cell Physiol.* 234, 8509–8521. doi:10.1002/jcp.27782

Feng, R.-M., Zong, Y.-N., Cao, S.-M., and Xu, R.-H. (2019). Current Cancer Situation in China: Good or Bad News from the 2018 Global Cancer Statistics? *Cancer Commun.* 39, 22. doi:10.1186/s40880-019-0368-6

- Gao, K., and Wu, J. (2019). National Trend of Gastric Cancer Mortality in China (2003-2015): A Population-Based Study. *Cancer Commun.* 39, 24. doi:10.1186/s40880-019-0372-x
- Ge, H., Yan, Y., Wu, D., Huang, Y., and Tian, F. (2018). Prognostic Value of PEG10 in Asian Solid Tumors: A Meta-Analysis. *Clinica Chim. Acta* 483, 197–203. doi:10.1016/j.cca.2018.04.041
- Grünebach, F., Erndt, S., Häntschel, M., Heine, A., and Brossart, P. (2008). Generation of Antigen-Specific CTL Responses Using RGS1 mRNA Transfected Dendritic Cells. *Cancer Immunol. Immunother.* 57, 1483–1491. doi:10.1007/s00262-008-0486-5
- Hong, S. A., Yoo, S. H., Lee, H. H., Sun, D. S., Won, H. S., Kim, O., et al. (2018). Prognostic Value of Dickkopf-1 and β -Catenin Expression in Advanced Gastric Cancer. *BMC Cancer* 18, 506. doi:10.1186/s12885-018-4420-8
- Janjigian, Y. Y., Bendell, J., Calvo, E., Kim, J. W., Ascierto, P. A., Sharma, P., et al. (2018). CheckMate-032 Study: Efficacy and Safety of Nivolumab and Nivolumab Plus Ipilimumab in Patients with Metastatic Esophagogastric Cancer. *J. Clin. Oncol.* 36, 2836–2844. doi:10.1200/jco.2017.76.6212
- Le, D. T., Uram, J. N., Wang, H., Bartlett, B. R., Kemberling, H., Eyring, A. D., et al. (2015). PD-1 Blockade in Tumors with Mismatch-Repair Deficiency. *N. Engl. J. Med.* 372, 2509–2520. doi:10.1056/nejmoa1500596
- Lee, H. S., Lee, H. E., Park, D. J., Kim, H.-H., Kim, W. H., and Park, K. U. (2012). Clinical Significance of Serum and Tissue Dickkopf-1 Levels in Patients with Gastric Cancer. *Clinica Chim. Acta* 413, 1753–1760. doi:10.1016/j.cca.2012.07.003
- Li, H., Xu, X., Liu, Y., Li, S., Zhang, D., Meng, X., et al. (2018). MMP7 Induces T-DM1 Resistance and Leads to the Poor Prognosis of Gastric Adenocarcinoma via a DKK1-Dependent Manner. *Anticancer Agents Med. Chem.* 18, 2010–2016. doi:10.2174/1871520619666181203111329
- Li, K., Zhang, A., Li, X., Zhang, H., and Zhao, L. (2021a). Advances in Clinical Immunotherapy for Gastric Cancer. *Biochim. Biophys. Acta Rev. Cancer* 1876, 188615. doi:10.1016/j.bbcan.2021.188615
- Li, S., Yang, H., Li, S., Zhao, Z., Wang, D., and Fu, W. (2021b). High Expression of Regulator of G-Protein Signalling 1 is Associated with the Poor Differentiation and Prognosis of Gastric Cancer. *Oncol. Lett.* 21, 322. doi:10.3892/ol.2021.12584
- Lin, B., Du, L., Li, H., Zhu, X., Cui, L., and Li, X. (2020). Tumor-Infiltrating Lymphocytes: Warriors Fight against Tumors Powerfully. *Biomed. Pharmacother.* 132, 110873. doi:10.1016/j.biopha.2020.110873
- Liu, Q.-R., Li, Y.-F., Deng, Z.-Q., and Cao, J.-Q. (2016). Prognostic Significance of Dickkopf-1 in Gastric Cancer Survival: A Meta-Analysis. *Genet. Test. Mol. Biomarkers* 20, 170–175. doi:10.1089/gtmb.2015.0154
- Llosa, N. J., Cruise, M., Tam, A., Wicks, E. C., Hechenbleikner, E. M., Taube, J. M., et al. (2015). The Vigorous Immune Microenvironment of Microsatellite Instable Colon Cancer is Balanced by Multiple Counter-Inhibitory Checkpoints. *Cancer Discov.* 5, 43–51. doi:10.1158/2159-8290.cd-14-0863
- Maher, J., and Davies, E. T. (2004). Targeting Cytotoxic T Lymphocytes for Cancer Immunotherapy. *Br. J. Cancer* 91, 817–821. doi:10.1038/sj.bjc.6602022
- Maleki Vareki, S. (2018). High and Low Mutational Burden Tumors Versus Immunologically Hot and Cold Tumors and Response to Immune Checkpoint Inhibitors. *J. Immunother. Cancer* 6, 157. doi:10.1186/s40425-018-0479-7
- McNamara, M. G., Jacobs, T., Lamarca, A., Hubner, R. A., Valle, J. W., and Amir, E. (2020). Impact of High Tumor Mutational Burden in Solid Tumors and Challenges for Biomarker Application. *Cancer Treat. Rev.* 89, 102084. doi:10.1016/j.ctrv.2020.102084
- Moratz, C., Kang, V. H., Druey, K. M., Shi, C.-S., Scheschonka, A., Murphy, P. M., et al. (2000). Regulator of G Protein Signaling 1 (RGS1) Markedly Impairs G α Signaling Responses of B Lymphocytes. *J. Immunol.* 164, 1829–1838. doi:10.4049/jimmunol.164.4.1829
- Raskov, H., Orhan, A., Christensen, J. P., and Gögenur, I. (2021). Cytotoxic CD8(+) T Cells in Cancer and Cancer Immunotherapy. *Br. J. Cancer* 124, 359–367. doi:10.1038/s41416-020-01048-4
- Rima, F. A., Hussain, M., Dewan, R. K., Haque, M. N., Sultana, T., Chowdhury, F., et al. (2020). Clinicopathologic Features of Gastric and Gastroesophageal Junction Adenocarcinoma. *Mymensingh Med. J.* 29, 195–201.
- Sharan Singh, S., Kumar, R., Singh Kushwaha, V., Bhatt, M. L. B. B., Singh, A., Mishra, A., et al. (2017). Expression of Radioresistant Gene PEG10 in OSCC Patients and its Prognostic Significance. *Asian Pac. J. Cancer Prev.* 18, 1513–1518. doi:10.22034/APJCP.2017.18.6.1513
- Taberero, J., Hoff, P. M., Shen, L., Ohtsu, A., Shah, M. A., Cheng, K., et al. (2018). Pertuzumab Plus Trastuzumab and Chemotherapy for HER2-Positive Metastatic Gastric or Gastro-Oesophageal Junction Cancer (JACOB): Final Analysis of a Double-Blind, Randomised, Placebo-Controlled Phase 3 Study. *Lancet Oncol.* 19, 1372–1384. doi:10.1016/s1470-2045(18)30481-9
- Taieb, J., Moehler, M., Boku, N., Ajani, J. A., Yañez Ruiz, E., Ryu, M.-H., et al. (2018). Evolution of Checkpoint Inhibitors for the Treatment of Metastatic Gastric Cancers: Current Status and Future Perspectives. *Cancer Treat. Rev.* 66, 104–113. doi:10.1016/j.ctrv.2018.04.004
- van Velzen, M. J. M., Derks, S., van Grieken, N. C. T., Haj Mohammad, N., and van Laarhoven, H. W. M. (2020). MSI as a Predictive Factor for Treatment Outcome of Gastroesophageal Adenocarcinoma. *Cancer Treat. Rev.* 86, 102024. doi:10.1016/j.ctrv.2020.102024
- Vrána, D., Matzenauer, M., Neoral, Č., Aujeský, R., Vrba, R., Melichar, B., et al. (2018). From Tumor Immunology to Immunotherapy in Gastric and Esophageal Cancer. *Int. J. Mol. Sci.* 20 (1), 13. doi:10.3390/ijms20010013
- Waldman, A. D., Fritz, J. M., and Lenardo, M. J. (2020). A Guide to Cancer Immunotherapy: From T Cell Basic Science to Clinical Practice. *Nat. Rev. Immunol.* 20, 651–668. doi:10.1038/s41577-020-0306-5
- Wall, J. A., Klempner, S. J., and Arend, R. C. (2020). The Anti-DKK1 Antibody DKN-01 as an Immunomodulatory Combination Partner for the Treatment of Cancer. *Expert Opin. Investig. Drugs* 29, 639–644. doi:10.1080/13543784.2020.1769065
- Wang, J., Chu, X. Q., Zhang, D., and Kong, D. F. (2018). Knockdown of Long Non-Coding RNA PEG10 Inhibits Growth, Migration and Invasion of Gastric Carcinoma Cells by Up-Regulating miR-3200. *Neoplasma* 65, 769–778. doi:10.4149/neo_2018_171204n794
- Xie, T., Pan, S., Zheng, H., Luo, Z., Tembo, K. M., Jamal, M., et al. (2018). PEG10 as an Oncogene: Expression Regulatory Mechanisms and Role in Tumor Progression. *Cancer Cell Int.* 18, 112. doi:10.1186/s12935-018-0610-3
- Zhang, D., He, W., Wu, C., Tan, Y., He, Y., Xu, B., et al. (2019). Scoring System for Tumor-Infiltrating Lymphocytes and its Prognostic Value for Gastric Cancer. *Front. Immunol.* 10, 71. doi:10.3389/fimmu.2019.00071
- Zhang, L., Wan, Y., Zhang, Z., Jiang, Y., Gu, Z., Ma, X., et al. (2021). IGF2BP1 Overexpression Stabilizes PEG10 mRNA in an m6A-Dependent Manner and Promotes Endometrial Cancer Progression. *Theranostics* 11, 1100–1114. doi:10.7150/thno.49345

Conflict of Interest: The authors declare that the research was conducted in the absence of any commercial or financial relationships that could be construed as a potential conflict of interest.

Publisher's Note: All claims expressed in this article are solely those of the authors and do not necessarily represent those of their affiliated organizations, or those of the publisher, the editors, and the reviewers. Any product that may be evaluated in this article, or claim that may be made by its manufacturer, is not guaranteed or endorsed by the publisher.

Copyright © 2022 Zhou, Hu, Hong, Wu, Zhang, Lai, Zhang and Wu. This is an open-access article distributed under the terms of the Creative Commons Attribution License (CC BY). The use, distribution or reproduction in other forums is permitted, provided the original author(s) and the copyright owner(s) are credited and that the original publication in this journal is cited, in accordance with accepted academic practice. No use, distribution or reproduction is permitted which does not comply with these terms.